Radar Observations of the Convective Process in the Clear Air – A Review

T. G. Konrad and J. S. Brennan
Applied Physics Laboratory Johns Hopkins University, Silver Spring, Maryland

Presented at the 12th OSTIV Congress, Alpine, USA (1970)

Introduction

Radar has been used as a remote probe to detect and study atmospheric processes such as precipitation and, to some extent, cloud formations for many years. In these cases, however, the radar returns are from particulate matter; water droplets or ice crystals. It has not been possible, until recently, to observe or «see» the structure and dynamics of the clear atmosphere with radar without these tracers.
Recent experiments have shown that the structure and dynamics of the visually clear atmosphere may be seen and studied using high-power, narrow-beam radars. Atmospheric conditions and processes of interest to the soaring pilot and soaring meteorologist such as the sea breeze front, inversions, and convective activity or thermals are observed routinely. The radar returns and patterns from these structures are quite distinctive and easily recognizable.
Convective activity in the clear air has been observed virtually throughout the year, in the summer over the land and during the late fall and early winter over the sea. The development of the covective field and the individual cells within the field has been followed in both time and space. Characteristics such as field growth rates, cell sizes, spacing etc. have been determined directly from the radar observation. In the past, these characteristics had to be deduced from secondary effects such as seagull flight patterns (Woodcock, 1942) from line measurements of some physical property such as temperature and/or moisture using instrumented aircraft (Grant, 1965; Warner and Telford, 1963, 1967) or from the observations of sailplane pilots (Yates, 1953). Using the radar as a remote probe, it is now possible to record and study both the statics and dynamics of the process directly.
This paper will review some of the findings resulting from the use of radar to study atmospheric processes in the optically clear atmosphere with primary emphasis on the observations of convection. All the illustrations and photographs of the radar returns from convective fields and cells were made in a visually clear atmosphere, except when specifically noted.
The work reported is part of a general program to study turbulent processes in the clear atmosphere. The research, hopefully, will lead to an understanding of the functional relationship between the refractive index structure of the atmosphere, the returned radar signal, and the velocity structure and, in turn, the nature of clear air turbulence.

Radar Returns from the Clear Air

No attempt will be made to review in any detail the theories concerning the reflection or scattering of electromagnetic energy by a refractively turbulent medium. However, an understanding of just what the radar «sees» is important to the interpretation of the radar returns and patterns discussed below.
Radar backscattering from clear air is caused by irregular, small-scale fluctuations in the radio refractive index produced by turbulent mixing. The refractive index fluctuations, in turn, are the result of variations in the physical properties of the air. Humidity variations are the principal contributors and, to a lesser extent, temperature variations. The effect of pressure gradients is small and generally ignored. Although fluctuations in the refractive index of many scales may well be present in any turbulent region, the radar is sensitive to and delineates only those regions where the scale of the fluctuations is one-half the radar wavelength (Tatarski, 1961; Kropfli et al., 1968). These small scale variations then act as tracers to outline or mark the larger scale motions.
In the convective process, a buoyant parcel of air rises through a stationary environment with turbulent mixing at the interfacing surfaces. The buoyancy of the rising parcel arises from either an excess of temperature or an excess of moisture, or some combination of the two. The turbulent mixing and resulting refractivity fluctuations are most pronounced at the outer edges or «skin» of the parcel and, therfore, the greater energy will be scattered from these regions. The sharpest gradients occur at the very top of the convective element and the strongest radar echoes occur at this point. On a Plan Position Indicator (PPI) which displays an essentially horizontal section through the cell, the characteristic doughnut or ring pattern results. On a Range Height Indicator (RHI), the cell appears as an inverted bowl or «U». These characteristic shapes or patterns of the radar returns from convective cells have been previously noted by Konrad (1968), Konrad and Kropfli (1968) and Hardy and Ottersten (1969) and are discussed in some detail in Konrad (1970).

Radar Equipment and Techniques

The radars used for all the observations reported here were the Joint Air Force-NASA (JAFNA) radars located on the Atlantic Coast at Wallops Island, Virginia. The JAFNA radar complex consists of three radars; X-band (3.2 cm), S-band (10.7 cm), and UHF (71.5 cm). The S-band and UHF radars have parabolic dish antennas of 60-foot diameter, producing 0.48 and 2.9 degree beamwidths, respectively. The X-band antenna is the inner 34 feet of the UHF antenna which produces an 0.21 degree beam. The S-band radar is a monopulse tracking radar. The X and UHF antenna is slaved to the S-band so that simultaneous observations of the same region of space at all wavelengths may be made within pulse volume limitations. The peak transmitter powers at X, S and UHF frequencies are 0.9, 3.0, and 6.0 megawatts, respectively. In short, the radars are very narrow beam and high power.
The multiwavelength capability of the JAFNA facility makes it possible to distinguish between various types of scattering mechanisms in the atmosphere on the basis of their wavelength dependence. Scatterers which are small relative to the radar wavelength (Rayleigh scatterers) such as raindrops or cloud droplets, produce a radar return which varies as the inverse fourth power of the wavelength. Present theories on the scattering of electromagnetic radiation from a turbulent medium partly substantiated by experiment indicate that the radar return ist proportional to the inverse one-third power of the wavelength. Thus, the scattering mechanism can be identified by the wavelength dependence of the return.
Photographs of PPI and RHI indicator presentations are used to display the radar returns from the clear-air atmospheric structures. The antennas are slewed very slowly, typically between 0.1 and 2.5 degrees per second, which provides some incoherent integration on the scope face and on the film. Stepped-elevation, rapid time se-

quence RHI and PPI photographs are used to record the spatial and temperal development of the convective field and the individual cells within the field. During many of the radar observations of convection an instrumented aircraft has been used to measure the physical properties of the cells and, in particular, those regions which produce the radar returns. The meteorological sensing instrumentation includes a Lyman-Alpha humidiometer to measure the water vapor content of the air, a three-axis hot wire anemometer to measure the three dimensional turbulent velocity structure, a fast response wire temperature probe, a pressure transducer, an accelerometer to measure the vertical accelerations, a vertical velocity sensor and a microwave cavity refractometer to measure the radio refractive index directly. Techniques have been developed for essentially simultaneous sampling of an air volume by radar and by the meteorological sensors aboard the aircraft.

Clear Air Convection Over Land

Convective activity in the clear air prior to any cloud formation is routinely observed by the radars over land throughout the spring, summer an early fall months. The development of the convective field has been followed from its initial formation through the growth state and the final dissipation. When a morning surface inversion is present due to nocturnal radiation cooling, the convective activity is initially confined to the depth of air lying below the inversion. During this period the radar returns from the convective activity are diffuse and mottled on PPI. Individual cells are identifiable only as hot-spots with ill-defined edges in an overall diffuse background. As time progresses and the inversion is elimenated and the first, small, doughnut-shaped cellular patterns appear on the PPIs.

At the onset of the growth stage the cells are small in both size (diameter) and vertical extent. The size of the cells making up the field increases with time and their tops extend to higher altitude. During this stage the cells typically appear well defined and organized in terms of their radar pattern, exhibiting the characteristic doughnut shape and inverted «U» discussed earlier. In some cases, the fluctuations in refractive index within the cell, as well as along the boundaries, are strong enough for the radar to detect and the cell appears on PPI photographs as a disc or a filled-in doughnut. When attenuation is added, however, the typical ring shaped patterns returns, indicating that the stronger echoes occur at the boundaries as expected.

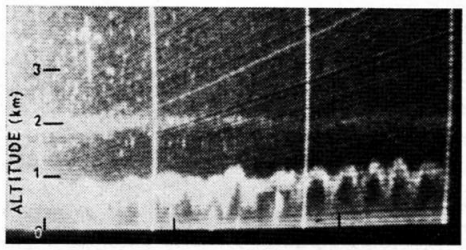

Fig. 1. RHI photographs through convective fields over land. Fig. 1a was taken while the sky was clear at 1330 EST on 30 July 1968 using the S-band radar. Fig. 1b was taken on 1 June 1966. At this time, cumulus clouds had formed at the tops of the cells shown.

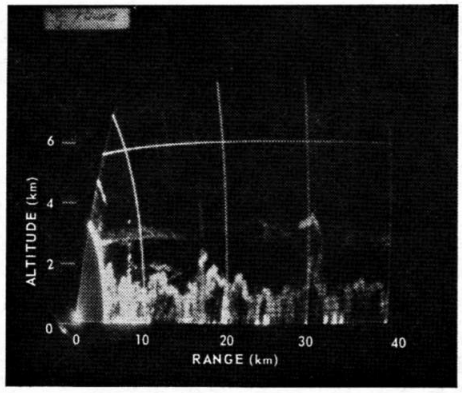

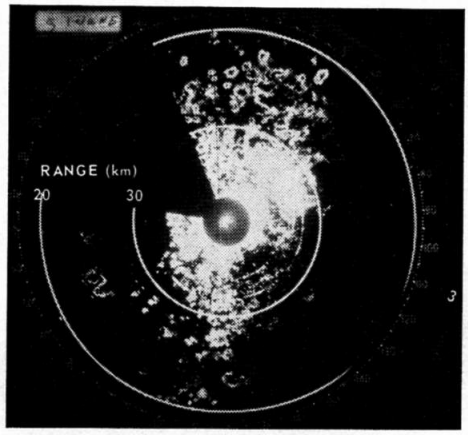

Fig. 2. PPI photographs through convective fields.

Fig. 2a is a full sweep PPI taken at 5 degrees elevation angle, 1 June 1966 at 1023 EST. The cells appear only over the land. The dark, echo free areas to the right and left side are water, the Atlantic and Chesapeake Bay. Fig. 2b is a PPI sector scan taken 5 June 1968 at 2 degrees elevation.

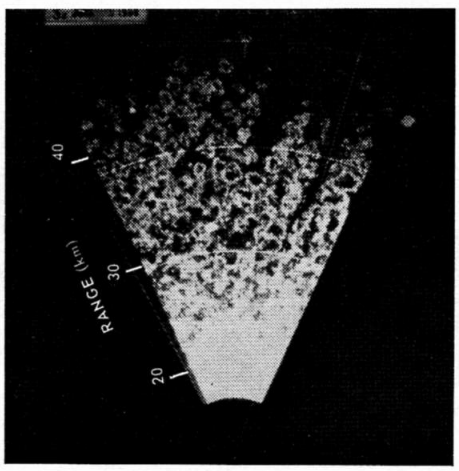

Figures 1 and 2 show typical examples of the radar returns from convective fields as seen on RHI and PPI respectively. The layer around 2.3 km shown in the RHI of figure 1b is a clear-air layer and not a cloud deck. Figure 1b was taken after cumulus clouds had formed with bases around 1.2 km. The clouds, then, are at the tops of the cells shown.

Figures 2a and b are PPI photographs and illustrate the ring shaped patterns of the cells. The convection is over land in clear air.

The well-defined, organized radar patterns shown in the above figures which characterize this development stage are not seen throughout the entire depth of the convective activity but are confined to the upper levels. As the day progresses the well defined cellular structures rise to greater altitudes. At the same time the lower altitudes, which previously were filled with the radar returns from convective cells, lose the well-defined patterns and the echoes become weak and diffuse. The PPI elevation angles must be continually increased to follow the cellular radar patterns.

Aircraft probes of the convective fields have shown the physical properties of the cells and the field. Next to the surface there is a superadiabatic layer. The buoyant elements are warm and lightly moist relative to their surroundings. The refractivity gradients are not large in this region; the temperature difference contributes little to the refractivity gradient and the moisture difference is generally small. Strong radar returns are not typically detected. As the elements rise, they cool by expansion and entrainment. The moisture contrast becomes larger as the cell rises. Momentum carries the cell or element past the equal temperature point, i.e., the point where the temperature of the cell is equal to that of the environment, and also past the zero buoyancy point into a region where the cell is cool and moist relative to the ambient air and has negative buoyancy. Simultaneous aircraft and radar observations show that the radar sees those regions where the convective element is cool and moist, i.e., the well defined radar patterns seen by radar are from those regions where the ascending elements are cool and moist. The aircraft probes have also found that the cells at the top of the convective field are not particularly turbulent. The most pronounced turbulence is found toward the mid-point of the depth of convective activity. Konrad (1970) and Katz (1970) discuss the above model of the convective process based on the radar and aircraft probes in considerable detail.

Time lapse movies, taken through convective fields during this stage, have shown the complexity of the in-

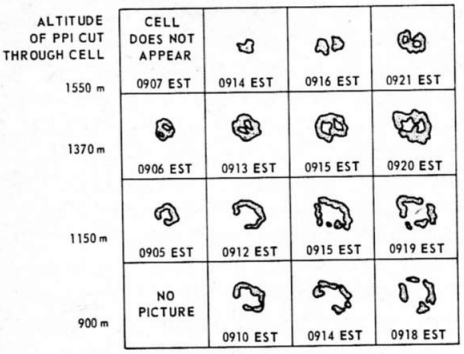

Fig. 3. Contour tracing of a single cell taken from time-sequence PPI pictures on 5 June 1968. The figure shows the growth with time of a single cell and the turreted (dual celled) top. At the lower elevations the cell grows in size but becomes progressively more fragmented.

ternal dynamics. In some cases an individual cell remains identifiable as a separate entity from its formation to its eventual dissipation when it reaches the top of the field. More commonly, however, cells are continually interacting and combining with other cells. Those forming in the lower levels grow rapidly and overtake the older, larger cells above. What appers to be a single cell at one elevation angle or altitude may, in fact, appear as two cells on higher or lower elevation cuts.

Cells often have turreted tops. This might well be expected in light of the observed growth of clouds. Figure 3 shows contour tracings of the same cell taken from a PPI sequence and illustrates several of the points discussed above. The cell growth is shown by the time sequence at several altitudes covering roughly 20 minutes. At the lower altitudes the cell appears singular and its pattern becomes progressively more unrecognizable with time as the top of the cell grows to higher levels. At higher elevations the cell appears two-headed. This situation tends to confuse any measurements of cell spacing, size distribution with height and, more fundamentally, the basic concept of a cell (or bubble or thermal) as a single entity.

In some cases, these time-lapse PPI observations have shown cells repeatedly appearing at the same location in the field. This would indicate that some fixed ground feature is acting as a source or a trigger to produce the thermal, but it has not yet been possible to identify specific ground sources based on the radar pictures. Considering the cell development model discussed above, however, this should not be too surprising. The cells drift with the mean wind, and by the time a buoyant element caused or triggered by some «hot spot» rises through the lower levels of the stable region, grows and becomes organized, its position with respect to the ground or location on the PPI presentation may bear little relation to the position of the ground feature. Since the rate of ascent of the convective element prior to its appearance on the PPI scope is unknown, it is difficult to extrapolate backward along some assumed path to the ground with any confidence.

The growth of individual cells in both altitude and diameter is quite rapid within the field during this stage. Hardy and Ottersten (1969) report individual cell tops rising from 0.5 to 1.5 m/sec with their diameters expanding at 0.5 to 1 m/sec. This growth rate of individual cell tops is considerably greater than the field-height growth rate discussed below and simply illustrates the diversity in dynamic scales contained in the overall convective process.

With regard to the cell diameters, figure 4 shows the growth with time for two altitude ranges on one particular day. Time sequence PPI pictures taken at 2- and 3-degree elevation angles were sectioned into the altitude increments shown. Within each altitude (or range) interval, the largest, smallest, and average cell diameters were measured for only those cells having well-defined, closed curve, doughnut or ring-shaped returns. As noted above, as time progresses and the altitude of the convection increases, the radar echoes from the cells at the lower levels become fragmented and unrecognizable. This occurred at approximately 1000 EST for the 750 to 1000 m altitude interval. Evidence of convection, however, was still strong at the higher altitudes. Again, this illustrates the movement of the radar patterns to higher altitudes with time. The sizes of cells, at a particular altitude and time, varies over a wide range. There is some indication on the 1000 to 1350 m increment figure, figure 4b, that the range of sizes increases with time. This appears consistent with the evidence and discussion above, in that when the convective field first reaches a given level, only the very tops are seen. As the field grows to higher altitudes, the original level is immersed in the convective activity and a wider range of cells (from newly formed, small cells to older, larger cells) are observed. That is, cells in various states of their individual development are passing through the particular altitude.

In general, the convective cells or thermal which make up the field appear randomly distributed over the land. This randomness extends throughout the depth of the convective field. However, under particular wind conditions, the tops of the convective cells are aligned in parallel rows along the mean wind direction. PPI scans through the lower regions do not show this alignment but rather the typical random distribution. These «thermal streets» in clear air were reported by Konrad (1968). Figures 5a and b show two examples of this alignment as seen by radar on PPI. The sector scan PPI, figure 5b, shows the cells very closely packed along the line. The wind conditions under which the cell alignment occurs were found to be generally consistent with those outlined by Kuettner (1959) for cloud streets; namely, the vertical wind profile is unidirectional but with a decided curvature in the wind speed.

As mentioned above, the field height or depth of convective activity increases with time. This field growth rate is not to be confused with the ascent rate of individual cells within the field. These grow at a much greater rate as noted by Hardy and Ottersten (1969). The growth of the convective field was

Fig. 4. The largest, smallest and average cell sizes are shown as a function of time for two altitudes. Only those cells with well defined, closed curve radar patterns were measured. The data are taken from stepped elevation PPI time series pictures at S-band (10.7 cm) on 5 June 1968.

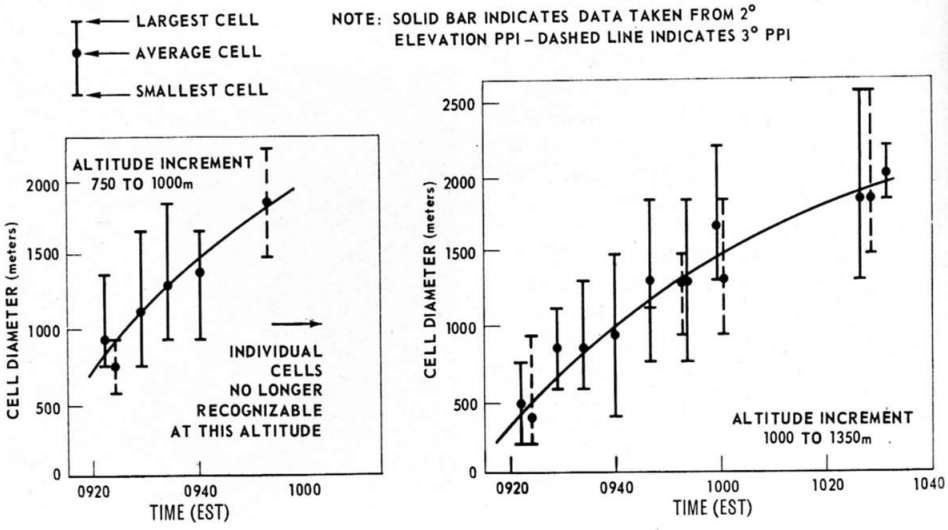

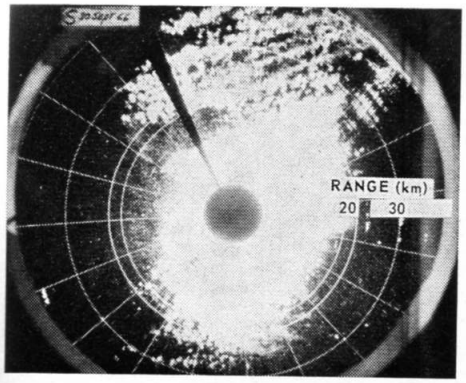

Fig. 5. PPI scans showing wind aligned convective cells (thermal streets). The rows of cells occur along the wind direction.

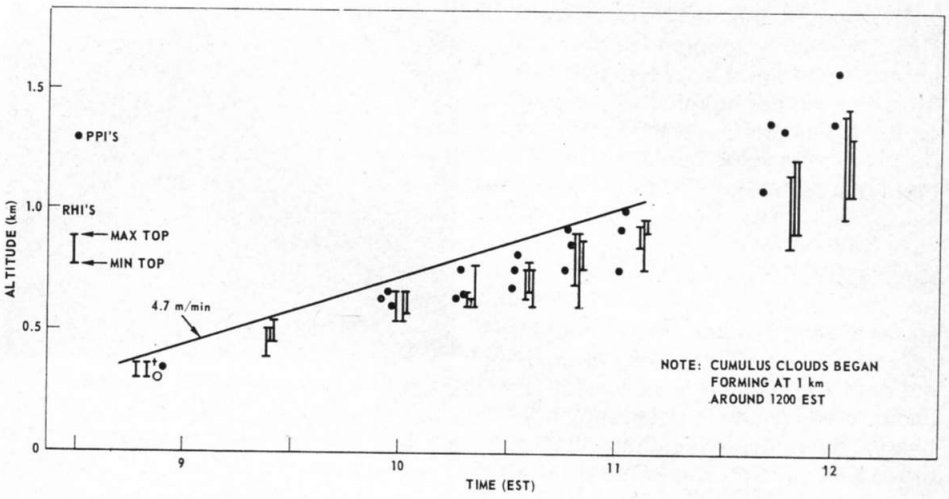

Fig. 6. The height of the convective field on 26 August 1969 measured from time sequence RHI and PPI photographs (see text). The line indicates the linear growth rate of approximately 4.7 m/min.

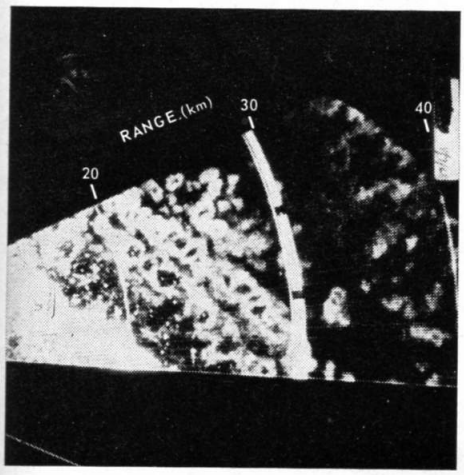

followed on ten days during 1968 and 1969; see Konrad (1970). Rapid time sequence RHIs and PPIs were used to follow the field development. An example of the results is shown in Figure 6. In nine of the ten cases examined, the field height was a linear function of time, i.e., the growth rate was constant. Values for the growth rate ranged from 4.5 to 6 m/min. The examination of field growth is continuing in an effort to establish a functional relationship between the growth rate and atmospheric conditions, e.g., temperature lapse rates, wind speeds etc.

The final stage in the clear air convective field development, as seen by radar, begins when the top of the field reaches either a strong elevated inversion or a condensing level. In the case of an elevated inversion, further growth of the field stops. The lower regions become mixed and finally only a single, layer-like, reflecting region remains. The height of this «layer» is slightly above the original inversion height. Figure 7 is an example of the radar pattern during this final stage. The absence of a radar echo below the layer does not imply that convection is no longer taking place. Most certainly convective activity continues until the surface heating stops. However, the air beneath this «layer» is so mixed that no refractivity gradients or fluctuations strong enough to produce a radar return exist. After the surface heating stops, the layer remains quite frequently is persistent enough to accentuate the temperature inversion the following morning.

Convection Over the Sea

During the late fall and early winter months the water temperature is warmer than the air temperature particularly in the case of outbreaks of Arctic air, which are typically followed at Wallops Island by winds from the north-west. Under these conditions convection over the sea has been observed by the radars. The observations have been made in the very early morning hours prior to sunrise when the land and air temperatures are at a minimum and the air-sea temperature contrast is greatest. The initial observations of over-sea convection by radar was reported by Konrad and Kropfli (1968). The sea temperature is generally constant within a degree or two for tens of miles to sea. With an off-shore wind, then the situation closely resembles an idealized, or laboratory model, i.e. cold air flowing over a cold surface (the land), across a well defined boundary (the shore-line) and onto a large, flat, uniformly heated surface (the sea). The observations by Konrad and Kropfli (1968) show the increase in the field height as a function of the distance from the shoreline as one might expect. They also found that the characteristics of the convective activity over the sea is essentially the same as that over land. That is, the cells appear randomly distributed but may be aligned under the wind conditions discussed above. Cell sizes are generally comparable. Aircraft flights as low as 100 feet over the sea have confirmed that these cells are also warm-and-moist in the lowest regions and cool-and-moist at the top of the radar patterns.

As one might expect, however, the progression or development of the convection is the reverse of that over land. As the sun rises and the land heats, the temperature contrast between air and sea decreases and the convection tends to die, hence, the observations prior to sunrise. Figure 8 shows a PPI picture taken in the morning of convective activity over the sea. This picture is part of a time sequence lasting approximately 7 hours.

The S-band radar being used for these experiments is coherent so that the Doppler velocity structure of the atmosphere may be measured. Convective cells over the sea have been examined to determine if any rotational motion

Fig. 7. RHI photograph showing the radar return which results when the convective field reaches a strong elevated inversion. The picture was taken 11 June 1970 at 1432 EST over land.

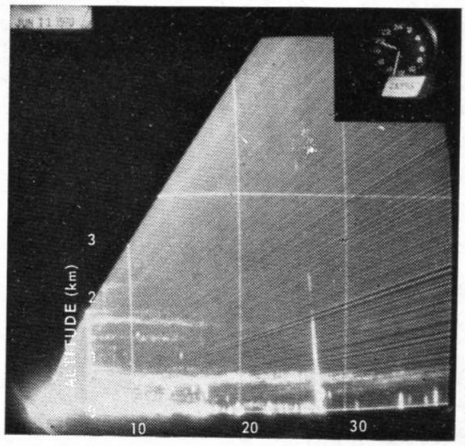

was present. If the cells rotate about a vertical axis the Doppler velocity should be different from one side to the other. No detectable shift, however, has been noted in the Doppler signal, within the velocity resolution of the radar system.

Conclusions

By far the most important result of the research, to date, have been to demonstrate the extent to which radar is capable and useful in detecting, identifying and studying the atmospheric processes which occur in the clear air. This new capability of radar to probe the clear air represents a significant advance in the technology of remote sensing and more specifically in the ability of the atmospheric scientist to directly observe and study the mesoscale dynamic processes in the atmosphere.

The convection studies reviewed above are but a small part of the overall research effort. However, the results to date have provided a much better understanding and appreciation of this mechanism which is so important in the air mass modification process.

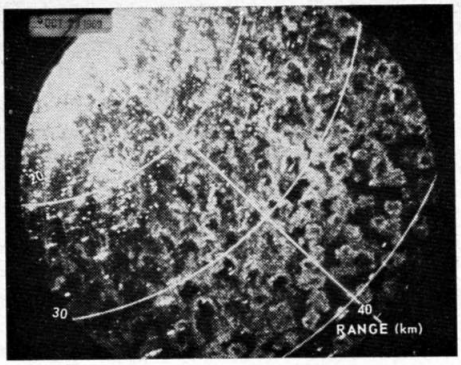

Fig. 8. Clear air convection over the sea on October 23, 1969 at 0800 EST. The PPI was taken at 1.0° elevation. All the area shown is over water. Convection was not present over land at this time.

Acknowledgements

This research has been supported by the Air Force Cambridge Research Laboratories and by the National Aeronautics and Space Administration.

References

1. Hardy, K. R. and Ottersten, H.: Radar Investigations of Convective Patterns in the Atmosphere (Jour. Atm. Sci. 26, 4, p. 666, 1969).
2. Katz, I.: Aircraft Soundings in Convection (APL/JHU Memo BPD70U-12, May 20, 1970).
3. Konrad, T. G.: The Alignment of Clear Air Convective Cells (Proc. Int. Conf. on Cloud Physics, Toronto 1968).
4. Konrad, T. G. and Kropfli, R. A.: Radar Observations of Clear Air Convection Over the Sea (Proc. 13th Radar Met. Conf. A.M.S., Boston 1968).
5. Konrad, T. G.: The Dynamics of the Convective Process in the Clear Air as Seen by Radar (Jour. Atm. Sci., November issue, 1970, accepted for publication).
6. Kropfli, R. A.; Katz, I.; Konrad, T. G., and Dobson, E.: Simultaneous Radar Reflectivity Measurements and Refractive Index Spectra in the Clear Atmosphere (Radio Science 3, 10, p. 991).
7. Kuettner, J.: The Band Structure of the Atmosphere (Tellus 11, 3, p. 267, 1959).
8. Tatarski, V. I.: Wave Propagation in a Turbulent Medium (McGraw Hill, 285, New York 1961).
9. Warner, J. and Telford, J. W.: Some Patterns of Convection in the Lower Atmosphere (Jour. Atm. Sci. 20, p. 313, 1963).
10. Warner, J. and Telford J. W.: Convection Below Cloud Base (Jour. Atm. Sci. 24, p. 374, 1967).
11. Woodcock, A. H.: Soaring Over the Open Sea (Sci. Monthly 55, p. 226, 1942).
12. Yates, A. H.: Atmospheric Convection; The Structure of Thermals Below Cloud Base (Q. Jour. Royal Met. Soc. 79, No. 341, 1953).